

Improvement in the Durability of Carbon Nanotube-Supported Ruthenium Catalysts by Coverage with Silica Layers

Takafumi Arike, Sakae Takenaka,* Hideki Matsune, and Masahiro Kishida*

Department of Chemical Engineering, Graduate School of Engineering, Kyushu University, 744 Moto-oka, Nishi-ku, Fukuoka 819-0395

Received April 2, 2010; E-mail: takenaka@chem-eng.kyushu-u.ac.jp

Carbon nanotube-supported Ru (Ru/CNT) catalysts were covered with silica layers to inhibit the aggregation of Ru particles as well as the detachment of Ru particles from the CNTs during catalytic reactions. Coverage of the Ru/CNT with silica was performed by the successive hydrolysis of 3-aminopropyltriethoxysilane and tetraethoxysilane in the presence of CNT-supported Ru metal precursors, followed by reduction with hydrogen at 623 K. The diameter of the Ru particles in the silica-coated Ru/CNT ranged from 1 to 3 nm. The Ru particles and the CNTs in the silica-coated catalysts were uniformly covered with silica layers a few nanometers thick. The size of the Ru particles in the silica-coated catalysts did not change appreciably after treatment at 873 K, while the metal particles in the Ru/CNT were seriously aggregated after treatment at 873 K. The silica-coated Ru/CNT catalyzed the CO hydrogenation and the 1-hexene hydrogenation, despite the coverage of Ru particles with silica. In addition, the silica-coated Ru catalysts showed high durability toward Ru detachment from the CNTs during the repeated hydrogenation of 1-hexene, whereas the catalysts without silica layers were deactivated because of Ru detachment. Therefore, coverage of the Ru/CNT catalysts with silica layers prevented the deactivation of the catalysts.

High-performance heterogeneous catalysts are increasing in demand for applications in clean technology and sustainable development. Precious metals such as Pt, Rh, and Ru have been used as catalytically active components in many catalytic reactions. For example, Pt metal is used as a catalyst in the cathodes for the oxygen reduction reaction and in the anodes for the hydrogen oxidation reaction in polymer electrolyte fuel cells (PEFCs).[1–3] Ru metal is frequently utilized for the hydroformylation of olefins[4–6] and for ammonia synthesis.[7–11] These precious metals show excellent catalytic performance in many reactions. However, precious metals are very expensive and scarce. Therefore, precious metals are usually supported on supports with large surface areas to enhance the catalytic activity of the metal, based on mass. Supported metal catalysts are conventionally prepared by the impregnation of supports in solutions containing the metal precursors, followed by the treatment of the metal precursors with reductants such as H_2 and $NaBH_4$.[12,13] These common methods tend to lead to a relatively weak interaction between metal particles and the supports. Therefore, the deactivation of supported metal catalysts is a serious problem that needs to be solved. The deactivation of the catalysts results from the aggregation of metal particles during the catalytic reactions because the reactions sometimes require severe conditions such as high temperatures and high pressures.[10–14] The sintering of metal particles occurs because of Ostwald ripening as well as the migration and coalescence of metal particles.[13] The driving force for the sintering of metal particles comes from the higher chemical potential of the metal atoms in small particles. To suppress the sintering of metal particles, a large surface area is an important requirement for the supports on which the metal particles are highly dispersed.[12] However, the sintering occurs easily in small particles. The strong interaction between metal particles and supports mitigates the sintering of the metal particles to some extent during reactions.[12,14] For example, Pt catalysts supported on Al_2O_3 for the purification of automobile emissions are exposed to severe conditions such as temperatures higher than 1000 K. Therefore, the Pt catalysts deactivate gradually with operation time because of the growth of Pt metal particles in size. The modification of Al_2O_3 supports with CeO_2 additives mitigates the aggregation of Pt at high temperature.[14] However, the interaction between metal particles and these additives is not always strong enough to prevent the sintering of metal particles. In addition, when supported metal catalysts are used for reactions in liquid solvents the metal particles detach easily from the supports, which also results in the deactivation of the catalysts.[15–20] This problem is caused by the physical detachment of the metal particles and the dissolution of the metal species during these reactions.[19] These detached metal particles also cause the sintering of the metal particles because they precipitate onto the supported metal particles. The detachment of metal particles from supports can be inhibited by the use of porous supports. For example, the Pd loading in Pd/SiO_2 was greatly decreased because of the detachment of metal during the hydrogenation of 1-hexene, whereas Pd metal particles that were enclosed in the mesopores of MCM-41 did not detach from their supports.[16,18] In addition, Ru particles embedded into templated porous carbon showed stable activity during the hydrogenation of benzene.[20,21] However, it is difficult to selectively support metal particles only in pore structures. In addition, the sintering of metal particles enclosed in these pores cannot be suppressed. Also, the methods that

Published on the web July 24, 2010; doi:10.1246/bcsj.20100095

require templates for the formation of porous structures in the catalysts are relatively complicated and impractical for industrial use.

Recently, we prepared multi-walled carbon nanotube (CNT)-supported Pt metal particles covered with a silica layer.[22,23] In these catalysts, Pt metal particles with diameters of 1–2 nm were supported onto CNTs and the outer surface of the metal particles and the CNTs was evenly covered by silica layers a few nanometers thick. In addition, we demonstrated that the silica-coated Pt/CNT catalysts showed high activity and excellent durability for the oxygen reduction reaction in PEFCs. In the present study, we used silica-coated catalysts for catalytic reactions in the gas and liquid phase. Ru metal was supported on CNTs in this study. Ru and Pt are very expensive and Ru is used industrially for the hydroformylation of olefins and for ammonia synthesis, as described earlier. However, Ru catalysts supported on carbon supports become deactivated because of the sintering and the detachment of Ru metal particles during ammonia synthesis at high temperatures and under high pressures, and during the repeated hydrogenation of benzene.[20,21] Covering Ru/CNT catalysts with silica layers is expected to mitigate the aggregation of Ru metal and the detachment of Ru metal from the CNTs during these reactions.

Experimental

Catalyst Preparation. Commercially available CNTs (supplied from Aldrich, outer diameter: 20–30 nm, inner diameter: 5–10 nm, length: 0.5–200 μm) were used as supports for Ru metal. CNTs were treated ultrasonically in an aqueous solution of H_2SO_4 and HNO_3 at 328 K for 2 h to oxidize the CNT surface.[2] The oxidized CNTs were immersed in an aqueous solution containing $RuCl_3$. The pH of this solution was adjusted to ca. 11 by adding aqueous NH_3 to deposit the Ru metal precursors onto the CNTs. After filtration, the samples were dispersed in water and then aqueous NH_3 and 3-aminopropyltriethoxysilane (APTES) were added to the solution at 333 K. The hydrolysis of tetraethoxysilane (TEOS) was subsequently performed at 333 K for 1 h. Finally, the sample was dried at 333 K in air, followed by exposure to an atmosphere of H_2 at 623 K for 3 h. The silica-coated Ru/CNT is denoted as SiO_2/Ru/CNT hereafter. A CNT-supported Ru catalyst (Ru/CNT) without a silica coating was also prepared using a similar preparation method to the preparation of the SiO_2/Ru/CNT. The oxidized CNTs were dispersed in an aqueous solution of $RuCl_3$ and then aqueous NH_3 was added to the solution to deposit Ru metal precursors onto the CNTs. The sample was dried at 333 K in air, followed by exposure to an atmosphere of H_2 at 623 K for 3 h.

Characterization of the Catalysts. The content of Ru and SiO_2 in the catalysts was determined by X-ray fluorescence spectroscopy (XRF) and inductively coupled plasma atomic emission spectrometry (ICP-AES). Transmission electron microscopy (TEM) images of the catalysts were recorded with a JEOL JEM-200CX instrument. The catalyst samples that were reduced with hydrogen at 623 K were dispersed in 2-propanol and the solution was mixed ultrasonically at room temperature. A part of this solution was dropped onto a grid before obtaining the TEM images.

X-ray absorption near-edge structure (XANES) and extended X-ray absorption fine structure (EXAFS) measurements were performed at the Photon Factory in the Institute of Materials Structure Science for High-Energy Accelerator Research Organization, Japan (proposal No. 2009G050). Ru K-edge XANES and EXAFS spectra were measured in a transmission mode at room temperature using beam line NW-10A with a Si(311) two crystal monochromator. The catalyst samples were reduced with hydrogen at 623 K before the XANES and EXAFS measurements. The catalyst samples were packed in a polyethylene bag under Ar. The EXAFS results were analyzed using an EXAFS analysis program, REX (Rigaku Co.). A Fourier transformation of the k^3-weighted EXAFS oscillations was performed over the k range from 3.5 to 15.5 $Å^{-1}$. Inversely Fourier transformed spectra for Fourier peaks were analyzed by a curve-fitting method using a phase shift and amplitude functions derived from FEFF 8.0.[24]

Reaction Conditions. The hydrogenation of CO and the hydrogenation of 1-hexene were performed over the Ru/CNT and the SiO_2/Ru/CNT. The hydrogenation of CO was performed using a conventional gas-flow reactor with a fixed catalyst bed at atmospheric pressure. Before the reaction, the catalysts were reduced with hydrogen at 623 K for 1 h. After catalyst pretreatment, a mixed gas of CO and hydrogen ($P(CO) = 15.2$ kPa, $P(H_2) = 30.3$ kPa) diluted with Ar was brought into contact with the catalysts. The hydrogenation of 1-hexene was performed with a batch-type reactor. An appropriate amount of Ru catalyst was dispersed in 1-hexene (5 mL) diluted with 2-propanol (95 mL). Subsequently, hydrogen (50 kPa) was diluted with He and introduced into the reactor. To evaluate the durability of the catalysts, the hydrogenation of 1-hexene was performed repeatedly using the same catalysts. After the hydrogenation of 1-hexene, the catalysts were recovered by filtration using a PTFE membrane filter (pore size: 0.1 μm), and then the recovered catalysts were dispersed again in 1-hexene diluted with 2-propanol.

Results and Discussion

Characterization of the Catalysts. Table 1 shows the Ru, SiO_2, and CNT content in the Ru/CNT and the SiO_2/Ru/CNT determined by XRF and ICP-AES. The Ru loading to the weight of the CNT supports in the SiO_2/Ru/CNT (9.7 wt%) was similar to that in the Ru/CNT (7.8 wt%). The amount of SiO_2 in the SiO_2/Ru/CNT was 42.3 wt%.

Figure 1 shows TEM images of the Ru/CNT and the SiO_2/Ru/CNT after reduction with hydrogen at 623 K. In TEM images (a) and (b) for the Ru/CNT, the Ru species seems to be supported on the CNT surfaces. The Ru species in the Ru/CNT are assignable to Ru metal by analyzing the XANES and EXAFS spectra for the catalysts, as described below. The size of the Ru metal particles in the Ru/CNT ranges from 1 to 5 nm

Table 1. Contents of Ru, SiO_2, and CNT in Ru/CNT and SiO_2/Ru/CNT

Sample	Loading/wt%		
	Ru	SiO_2	Carbon
Ru/CNT	7.8	—	92.2
SiO_2/Ru/CNT	5.6	42.3	52.1

and these metal particles are uniformly supported on the surface of the CNT. TEM images (c) and (d) for the SiO_2/Ru/CNT show that the Ru metal particles are present on the CNTs and that the Ru metal particles as well as the CNTs seem to be evenly covered with silica. The size of the Ru metal particles in the SiO_2/Ru/CNT is ca. 1 nm, which is smaller than that in the Ru/CNT and the Ru particles are densely supported on the outer surface of the CNTs. The SiO_2/Ru/CNT was treated with hydrogen at 623 K after coverage of the CNT-supported Ru metal precursors with silica. The silica layers that wrapped the Ru metal precursors should prevent the aggregation of Ru species during the treatment with hydrogen at 623 K. Therefore, the size of the Ru metal particles in the SiO_2/Ru/CNT was smaller than that in the Ru/CNT. In addition, the successive hydrolysis of APTES and TEOS on the CNTs with the Ru precursors resulted in an even coverage of the Ru/CNT with silica layers. It has been reported that APTES was strongly adsorbed on CNTs through a strong interaction between the amino groups in APTES and the surfaces of the CNTs.[25] During the successive hydrolysis of APTES and TEOS, silica primary particles formed from the hydrolysis of TEOS were preferentially deposited on APTES, which had previously been adsorbed onto the CNTs. Therefore, the Ru/CNT was evenly coated with silica layers by the successive hydrolysis of APTES and TEOS.

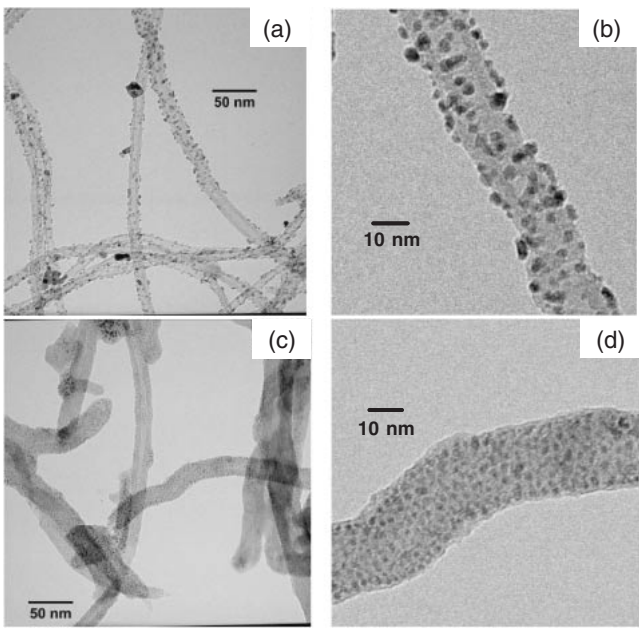

Figure 1. TEM images of Ru/CNT (a and b), and SiO_2/Ru/CNT (c and d) after reduction at 623 K.

To examine the chemical state and structure of the Ru species in the Ru/CNT and the SiO_2/Ru/CNT, Ru K-edge XANES and EXAFS for the catalysts were measured. Figure 2a shows XANES spectra of the Ru/CNT, SiO_2/Ru/CNT, and reference samples (Ru metal and RuO_2). Ru K-edge XANES spectra are sensitive to the oxidation states of Ru, as explained by the spectra of Ru metal and RuO_2.[26,27] The XANES spectrum of the Ru/CNT is similar to that of Ru metal. Therefore, Ru species in the Ru/CNT are present as Ru metal. On the other hand, the threshold at around 22100 eV in the XANES spectrum of SiO_2/Ru/CNT was located in a similar position to that of the spectrum of Ru metal. In addition, two broad peaks were observed at 22120 and 22150 eV in the XANES spectrum of SiO_2/Ru/CNT, similarly to those in the spectrum of Ru metal. These results suggest that most of the Ru species in SiO_2/Ru/CNT were present as Ru metal. However, the peak intensity at 22120 eV in the XANES spectrum of SiO_2/Ru/CNT was stronger than that of Ru metal. This is because some Ru species in the SiO_2/Ru/CNT were oxidized, as shown by the XANES spectrum of RuO_2. As described earlier, the Ru metal particles in the SiO_2/Ru/CNT were evenly covered with silica layers. A portion of the surface Ru species in the Ru metal particles within the SiO_2/Ru/CNT was oxidized because of the interaction between silica and the Ru metal particles. Figure 2b shows Fourier transforms of k^3-weighted Ru K-edge EXAFS spectra (RSFs; radial structural functions) for the Ru/CNT, SiO_2/Ru/CNT, and reference samples. Three peaks are present at 2.4, 3.5, and 4.3 Å in the spectra for Ru metal, the Ru/CNT, and the SiO_2/Ru/CNT,

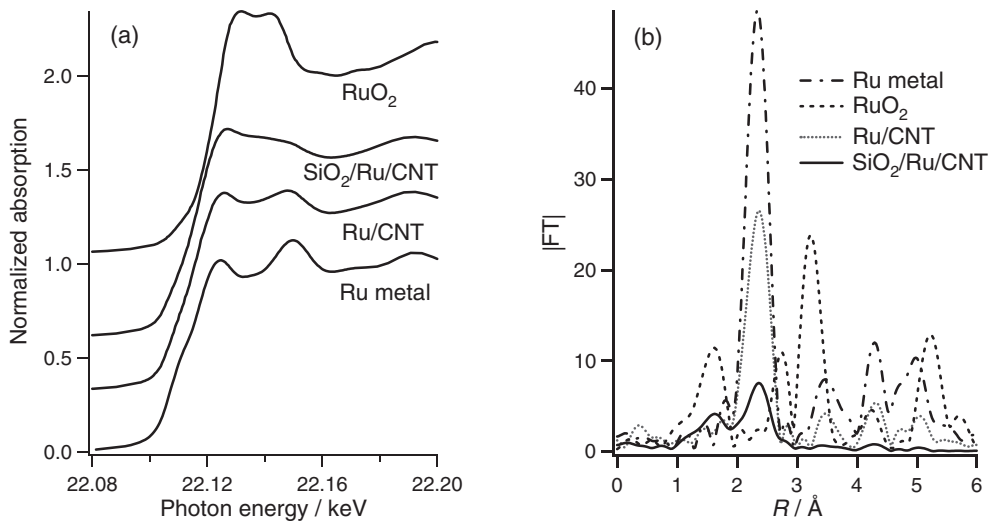

Figure 2. Ru K-edge XANES spectra (a) and Fourier transforms of k^3-weighted Ru K-edge EXAFS spectra (b) for Ru/CNT, SiO_2/Ru/CNT, Ru metal, and RuO_2.

Table 2. Structural Parameters of Ru Species in Ru/CNT and SiO_2/Ru/CNT Catalysts Estimated by Curve-Fitting Analyses of EXAFS Spectra

Sample	Shell	CN[a)]	R[b)]/Å	DW[c)]/Å
Ru/CNT	Ru–Ru	8.3 (±0.3)	2.66	0.072
SiO_2/Ru/CNT	Ru–Ru	4.2 (±0.4)	2.64	0.091
	Ru–O	1.4 (±0.3)	2.03	0.068

a) Coordination number. b) Interatomic distance. c) Debye–Waller factor.

although the peak intensity in the SiO_2/Ru/CNT was much smaller than that for the other samples. These results indicate that most of the Ru species in the Ru/CNT and the SiO_2/Ru/CNT are present as Ru metal. The peak intensity of the EXAFS spectra for any metal sample depends on the metal's crystallite size, that is, the peak intensity becomes stronger as the crystallite size of the metal increases.[28] Thus, the crystallite size of the Ru metal in the SiO_2/Ru/CNT should be smaller than that in the Ru/CNT.

To further clarify the structure of the Ru species in the Ru/CNT and the SiO_2/Ru/CNT, curve-fitting was carried out for the Ru K-edge EXAFS spectra. Table 2 shows the results of the curve-fitting analyses for the Ru K-edge EXAFS spectra. The peaks in the R range from 1.0–3.0 Å in the RSF (radial structural functions) were inversely Fourier-transformed and the EXAFS spectrum thus obtained was fitted in the k range from 4–15 $Å^{-1}$. The EXAFS spectrum of the Ru/CNT could be fitted using a shell of the Ru–Ru bond only and the coordination number was 8.3. In contrast, the EXAFS spectrum for the SiO_2/Ru/CNT could be fitted using a shell of the Ru–O bond and a shell of the Ru–Ru bond. The low coordination number of the Ru–Ru bond suggested the presence of Ru metal with a smaller crystallite size in the SiO_2/Ru/CNT than that in the Ru/CNT. The presence of Ru–O in the SiO_2/Ru/CNT implied a strong interaction of surface Ru atoms in the Ru metal particles with silica, although the catalysts had been reduced with hydrogen at 623 K before the EXAFS spectra measurements. A part of surface Ru atoms on Ru metal particles in SiO_2/Ru/CNT was strongly interacted with silica layers through Si–O–Ru bonds. In addition, some Ru species in SiO_2/Ru/CNT would be stabilized as highly dispersed RuO_x species and small Ru metal clusters in silica layers. We have reported the preparation of Co metal particles enclosed in the spherical silica particles.[29] Some Co species in the catalysts, which had been treated at 1073 K, were present as atomically dispersed CoO_x species in silica body, although most Co species in the catalysts were reduced to the metallic states. The highly dispersed Ru species in the SiO_2/Ru/CNT could not be observed in TEM images of the catalysts. Some of the highly dispersed Ru species in SiO_2/Ru/CNT were reduced during the treatment of the catalysts at 873 K, as described below.

To examine the durability to sintering of the Ru particles in the Ru/CNT and the SiO_2/Ru/CNT, these samples were treated at 873 K under Ar for 5 h. Figures 3a and 3b show TEM images of the Ru/CNT after treatment at 873 K. In the TEM images, Ru metal particles larger than 10 nm are easily found, while the size of Ru metal in the Ru/CNT treated at 623 K ranged from 1 to 5 nm (Figures 1a and 1b). Based on these

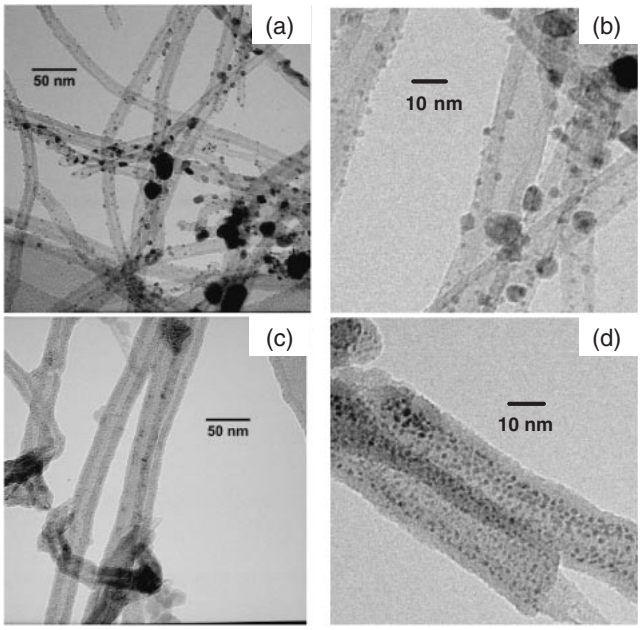

Figure 3. TEM images of Ru/CNT (a and b), and SiO_2/Ru/CNT (c and d) after treatment at 873 K.

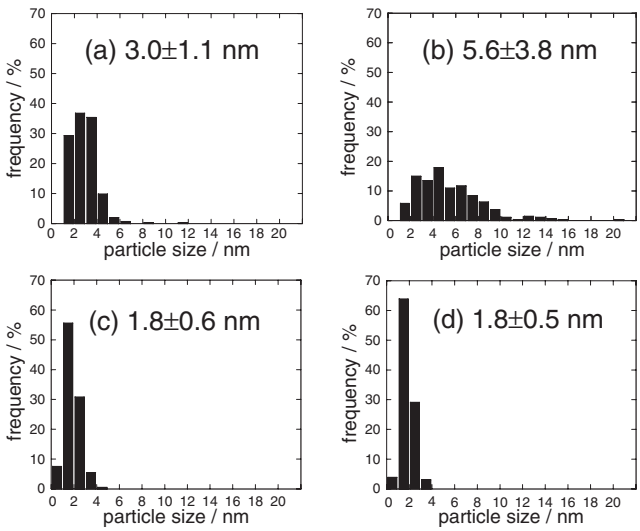

Figure 4. The distribution of Ru particle size for Ru/CNT and SiO_2/Ru/CNT. (a), Ru/CNT after treatment at 623 K; (b), Ru/CNT after treatment at 873 K; (c), SiO_2/Ru/CNT after treatment at 623 K; and (d), SiO_2/Ru/CNT after treatment at 873 K.

TEM images, the size distribution of the Ru particles was evaluated. The results are shown in Figure 4. The size of the Ru metal particles in the Ru/CNT treated at 623 K ranged from 1 to 5 nm and the average size was estimated to be 3.0 nm. After treatment of the Ru/CNT at 873 K the fraction of Ru metal particles with diameters from 1 to 4 nm decreased significantly and the fraction of particles with diameters larger than 6 nm increased. Therefore, the Ru metal particles in the Ru/CNT were easily aggregated by treatment at high temperature. In contrast, Ru metal particles in the SiO_2/Ru/CNT did not grow in size during treatment at 873 K. As shown in

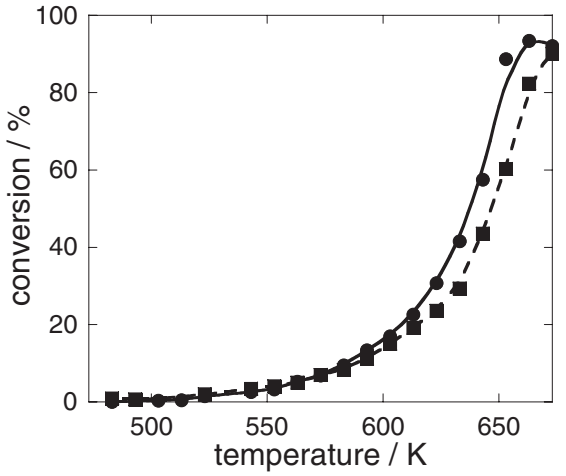

Figure 5. Change of CO conversion with temperatures in CO hydrogenation over Ru/CNT (●) and SiO_2/Ru/CNT (■).

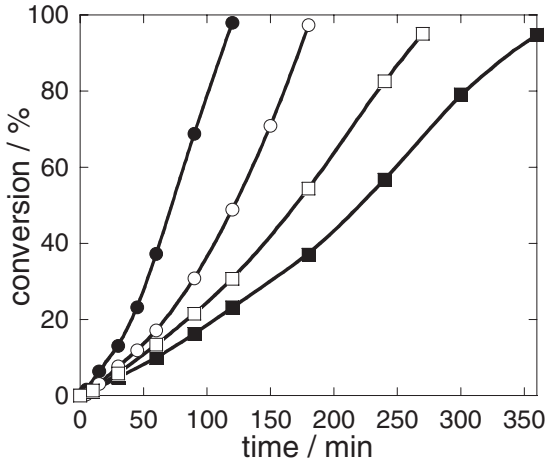

Figure 6. Change of the conversion of 1-hexene with time in the hydrogenation of 1-hexene over Ru/CNT and SiO_2/Ru/CNT. ●, Ru/CNT treated at 623 K; ○, Ru/CNT treated at 873 K; ■, SiO_2/Ru/CNT treated at 623 K; and □, SiO_2/Ru/CNT treated at 873 K.

Figures 3c and 3d, Ru metal particles of 1–2 nm in diameter were present in the silica layer and the size was very similar to that of the SiO_2/Ru/CNT treated at 623 K (Figures 1c and 1d). In addition, Ru metal particles and CNTs were evenly covered with silica layers after treatment at 873 K, indicating that the silica layers in the SiO_2/Ru/CNT were also stable at high temperatures. Figures 4c and 4d also show that the size distribution and the average size of Ru metal particles in the SiO_2/Ru/CNT did not change during treatment at 873 K. Thus, the coverage of the Ru/CNT with silica layers improved the sintering durability of the Ru metal particles.

Catalytic Activity and Durability. Figure 5 shows the change in CO conversion with reaction temperature during CO hydrogenation over the Ru/CNT and SiO_2/Ru/CNT catalysts. The amount of catalyst placed in the reactors was such that the Ru content was equivalent for both the reactions. CH_4 was mainly produced by CO hydrogenation and a trace amount of C_2H_6 and C_3H_8 was also formed over the Ru/CNT and the SiO_2/Ru/CNT. The conversion of CO over Ru/CNT gradually increased with temperature as shown in Figure 5. It should be noted that the catalytic activity of the SiO_2/Ru/CNT was very similar to that of the Ru/CNT, despite the coverage of the Ru metal with a silica layer. Reactant molecules such as CO and H_2 diffuse to the surface of the Ru metal in the SiO_2/Ru/CNT because the silica layers have a porous structure. Therefore, the SiO_2/Ru/CNT showed high activity for the hydrogenation of CO.

To examine whether the silica-coated catalyst could be applied to a liquid phase reaction, the hydrogenation of 1-hexene was performed over the Ru/CNT and SiO_2/Ru/CNT catalysts. Figure 6 shows the change in 1-hexene conversion with time during the hydrogenation of 1-hexene over the Ru/CNT and SiO_2/Ru/CNT catalysts. The reactions were performed over the catalysts reduced with H_2 at 623 K as well as the catalysts after the same H_2 reduction, followed by treatment at 873 K under Ar. The amount of these catalysts loaded into the reactors was such that the Ru content was equivalent in all reactions. The SiO_2/Ru/CNT treated at 623 K could catalyze the hydrogenation of 1-hexene with similar results compared to the Ru/CNT, despite the coverage of Ru metal with silica layers. However, the catalytic activity of the SiO_2/Ru/CNT was much lower than that of the Ru/CNT. The slow diffusion rate of 1-hexene in the silica layers of the SiO_2/Ru/CNT causes the low catalytic activity of the SiO_2/Ru/CNT. The catalytic activity of the Ru/CNT decreased after treatment at 873 K. As described earlier, Ru metal particles in the Ru/CNT aggregate during treatment at 873 K. An increase in the particle size of Ru metal in the Ru/CNT should bring about a decrease in catalytic activity. In contrast, the catalytic activity of the SiO_2/Ru/CNT was enhanced after treatment at 873 K. This was due to a change in the properties of the silica and a reduction of Ru oxide in the catalysts during treatment at 873 K. Treatment of the SiO_2/Ru/CNT at high temperature caused the dehydration of silica.[30] During this dehydration, silica undergoes a hydrophilic to hydrophobic transformation. The hydrophobic surface of the catalyst should enhance the diffusion of 1-hexene in the silica layers that are wrapped around the Ru metal. The reduction of Ru species in the SiO_2/Ru/CNT during the treatment at 873 K was shown in XANES spectra in Figure 7. The peak intensity at around 22120 eV in XANES spectra of SiO_2/Ru/CNT became lower with an increase in the treatment temperature of the catalysts. The XANES spectrum of SiO_2/Ru/CNT treated at 873 K was consistent with that of Ru metal. Thus, oxidized Ru species in SiO_2/Ru/CNT which had been reduced with hydrogen at 623 K were reduced during the treatment of the catalysts at 873 K. Carbon atoms in the CNTs likely act as reductants for Ru oxides to form Ru metal. Therefore, the catalytic activity of the SiO_2/Ru/CNT for the hydrogenation of 1-hexene was improved because of the high temperature treatment.

The durability of Ru/CNT treated at 623 K and the SiO_2/Ru/CNT after treatment at 873 K for the repeated hydrogenation of 1-hexene was evaluated. Figure 8 shows the change in 1-hexene conversion with time in the repeated hydrogenation of 1-hexene over the Ru/CNT and SiO_2/Ru/CNT catalysts. In the reactions over the Ru/CNT catalysts, the

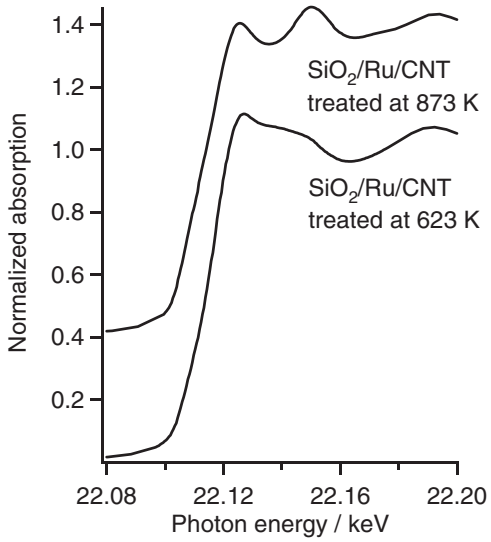

Figure 7. Ru K-edge XANES spectra for SiO_2/Ru/CNT treated at 623 and 873 K.

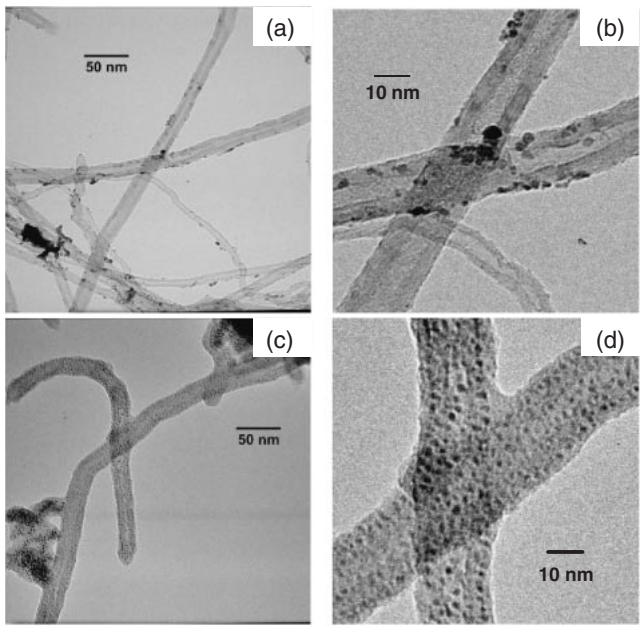

Figure 9. TEM images of Ru/CNT (a and b), and SiO_2/Ru/CNT (c and d) after the 5th runs.

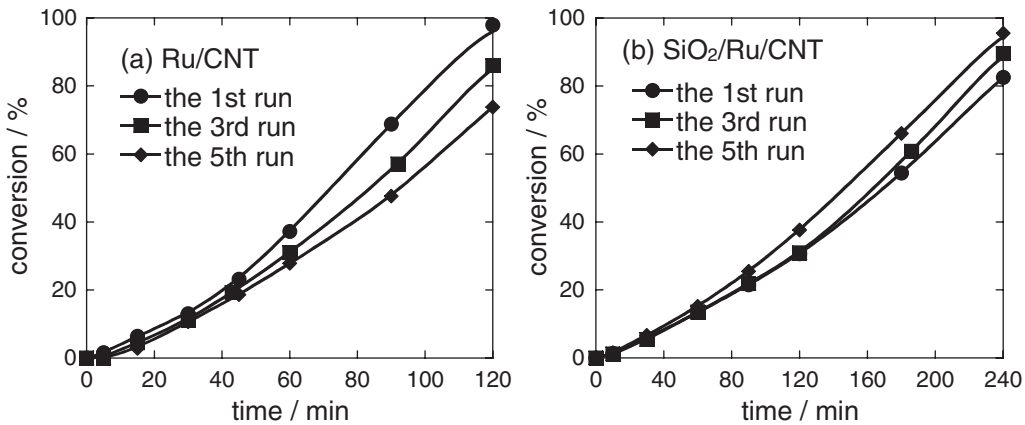

Figure 8. Change of 1-hexene conversion with time in the repeated hydrogenation of 1-hexene over Ru/CNT and SiO_2/Ru/CNT.

hydrogenation rate of 1-hexene gradually decreases with the repetition of the reactions. It is likely that the Ru particles in the Ru/CNT are detached from the CNTs during these reactions. In contrast, the catalytic activity of the SiO_2/Ru/CNT did not decrease during the repeated hydrogenation of 1-hexene. Therefore, the coverage of the Ru/CNT with silica layers improved the durability of the catalysts to the repeated reactions. The silica layer that was wrapped around the Ru metal may prevent the detachment of the Ru metal from the CNTs. Figure 9 shows the TEM images of the used Ru/CNT (Figures 9a and 9b) and the used SiO_2/Ru/CNT (Figures 9c and 9d). These TEM images were measured after the 5th run of the repeated 1-hexene hydrogenation. In TEM images of the used Ru/CNT, Ru metal particles were present on the surface of the CNTs. However, the density of the Ru particles on the CNTs in the used Ru/CNT was lower than that of the fresh Ru/CNT (Figures 1a and 1b). On the other hand, Ru metal particles were present in the silica bodies in the used SiO_2/Ru/CNT, which was similar to that found for the fresh SiO_2/Ru/CNT. It is important to note that the number and density of the Ru particles in the SiO_2/Ru/CNT did not change after the 5th run. This result indicates that coverage of the Ru/CNT with silica layers prevents the detachment of Ru metal particles from the CNTs during catalytic reactions.

To further explain the loss of Ru metal in the Ru/CNT and the SiO_2/Ru/CNT during the repeated hydrogenation of 1-hexene, the amount of Ru detached and/or leached from these catalysts in each run was measured. After each run over the catalysts, the reaction mixture was filtered to recover the catalysts and then the filtrate obtained was analyzed by ICP. Figure 10 shows the amount of Ru lost from the fresh catalysts. The amount of Ru lost from the Ru/CNT increased gradually with the repeated runs and 12% of the Ru in the catalysts was removed after the 5th run. In contrast, no Ru species was detected in the filtrate after the reaction over the SiO_2/Ru/CNT. These results clearly indicated that coverage of the Ru/

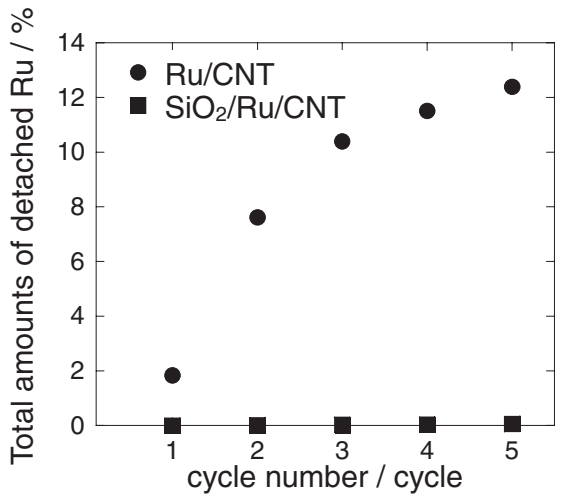

Figure 10. Change of Ru loading in Ru/CNT and SiO_2/Ru/CNT during the repeated hydrogenation of 1-hexene.

CNT with silica layers prevents the detachment and/or dissolution of Ru metal particles from the CNT. Therefore, the SiO_2/Ru/CNT showed high durability during the repeat reactions.

Conclusion

To improve the stability of CNT-supported Ru catalysts, they were covered with silica layers. By the successive hydrolysis of 3-aminopropyltriethoxysilane and tetraethoxysilane, the Ru/CNT was evenly covered with thin silica layers. Coverage of the Ru/CNT with these silica layers improved its durability toward Ru sintering at high temperatures. The silica-coated Ru/CNT catalysts showed high activity for the hydrogenation of CO and 1-hexene. In addition, coverage of the Ru/CNT with silica layers prevented the detachment of Ru metal particles during the repeated hydrogenation of 1-hexene.

This work was supported by a Grant-in-Aid for JSPS research Fellowships for Young Scientists and by a Grant-in-Aid for the Global COE Program, "Science for Future Molecular Systems" from the Ministry of Education, Culture, Sports, Science and Technology of Japan.

References

1 N. Rajalakshmi, H. Ryu, M. M. Shaijumon, S. Ramaprabhu, *J. Power Sources* **2005**, *140*, 250.
2 Y. Xing, *J. Phys. Chem. B* **2004**, *108*, 19255.
3 Z. Liu, X. Lin, J. Y. Lee, W. Zhang, M. Han, L. M. Gan, *Langmuir* **2002**, *18*, 4054.
4 Y. Zhang, K. Nagasaka, X. Qiu, N. Tsubaki, *Appl. Catal., A* **2004**, *276*, 103.
5 S. Pien, S. S. C. Chuang, *J. Mol. Catal.* **1991**, *68*, 313.
6 M. E. Halttunen, M. K. Niemelä, A. O. I. Krause, A. I. Vuori, *J. Mol. Catal. A: Chem.* **1996**, *109*, 209.
7 I. Rossetti, N. Pernicone, L. Forni, *Appl. Catal., A* **2001**, *208*, 271.
8 I. Rossetti, N. Pernicone, L. Forni, *Catal. Today* **2005**, *102–103*, 219.
9 Z. Kowalczyk, S. Jodzis, W. Raróg, J. Zieliński, J. Pielaszek, *Appl. Catal., A* **1998**, *173*, 153.
10 Z. Song, T. Cai, J. C. Hanson, J. A. Rodriguez, J. Hrbek, *J. Am. Chem. Soc.* **2004**, *126*, 8576.
11 Q. Xu, J. Lin, J. Li, X. Fu, Z. Yang, W. Guo, D. Liao, *J. Mol. Catal. A: Chem.* **2006**, *259*, 218.
12 K. Hayashi, T. Horiuchi, K. Suzuki, T. Mori, *Catal. Lett.* **2002**, *78*, 43.
13 A. K. Datye, Q. Xu, K. C. Kharas, J. M. McCarty, *Catal. Today* **2006**, *111*, 59.
14 A. Martínez-Arias, J. M. Coronado, R. Cataluña, J. C. Conesa, J. Soria, *J. Phys. Chem. B* **1998**, *102*, 4357.
15 J. Chen, A. N. Vasiliev, A. P. Panarello, J. G. Khinast, *Appl. Catal., A* **2007**, *325*, 76.
16 J. Panpranot, K. Pattamakomsan, J. G. Goodwin, Jr., P. Praserthdam, *Catal. Commun.* **2004**, *5*, 583.
17 M. Besson, P. Gallezot, *Catal. Today* **2003**, *81*, 547.
18 J. Panpranot, K. Pattamakomsan, P. Praserthdam, J. G. Goodwin, Jr., *Ind. Eng. Chem. Res.* **2004**, *43*, 6014.
19 W. Deng, X. Tan, W. Fang, Q. Zhang, Y. Wang, *Catal. Lett.* **2009**, *133*, 167.
20 S. Miao, Z. Liu, B. Han, J. Huang, Z. Sun, J. Zhang, T. Jiang, *Angew. Chem., Int. Ed.* **2006**, *45*, 266.
21 F. Su, F. Y. Lee, L. Lv, J. Liu, X. N. Tian, X. S. Zhao, *Adv. Funct. Mater.* **2007**, *17*, 1926.
22 S. Takenaka, H. Matsumori, K. Nakagawa, H. Matsune, E. Tanabe, M. Kishida, *J. Phys. Chem. C* **2007**, *111*, 15133.
23 S. Takenaka, H. Matsumori, T. Arike, H. Matsune, M. Kishida, *Top. Catal.* **2009**, *52*, 731.
24 D. A. Dimitrov, A. L. Ankudinov, A. R. Bishop, S. D. Conradson, *Phys. Rev. B* **1998**, *58*, 14227.
25 Q. Fu, C. Lu, J. Liu, *Nano Lett.* **2002**, *2*, 329.
26 T. Tanaka, H. Yamashita, R. Tsuchitani, T. Funabiki, S. Yoshida, *J. Chem. Soc., Faraday Trans. 1* **1988**, *84*, 2987.
27 W. C. Ketchie, E. P. Maris, R. J. Davis, *Chem. Mater.* **2007**, *19*, 3406.
28 S. D. Jackson, J. Willis, G. D. Mclellan, G. Webb, M. B. T. Keegan, R. B. Moyes, S. Simpson, P. B. Wells, R. Whyman, *J. Catal.* **1993**, *139*, 191.
29 S. Takenaka, Y. Orita, H. Matsune, E. Tanabe, M. Kishida, *J. Phys. Chem. C* **2007**, *111*, 7748.
30 L. T. Zhuravlev, *Colloids Surf., A* **2000**, *173*, 1.